doi: 10.1111/j.1365-3121.2009.00896.x

Active crustal shortening in NE Syria revealed by deformed terraces of the River Euphrates

Mohammad Abou Romieh,[1] Rob Westaway,[2] Mohamad Daoud,[1] Yousef Radwan,[3] Rayan Yassminh,[1] Ahlam Khalil,[1] Abeer al-Ashkar,[4,8] Susan Loughlin,[5] Katherine Arrell[6] and David Bridgland[7]

[1]*National Earthquake Center, Rasheed Karameh Street, Al-Adawi, Damascus, Syria;* [2]*MCT, The Open University, Abbots Hill, Gateshead NE8 3DF, UK, also at IRES, Newcastle University, Newcastle-upon-Tyne NE1 7RU, UK;* [3]*Syrian Atomic Energy Commission, Damascus, Syria;* [4]*Department of Geology, Damascus University, Damascus, Syria;* [5]*British Geological Survey, Murchison House, West Mains Road, Edinburgh EH9 3LA, UK;* [6]*Department of Geography, Leeds University, Leeds LS2 9JT, UK;* [7]*Department of Geography, Durham University, Durham DH1 3LE, UK;* [8]*Present address: Institut de Physique du Globe de Paris, 4 Place Jussieu, 75252 Paris Cedex 05, France*

ABSTRACT

The Africa–Arabia plate boundary comprises the Red Sea oceanic spreading centre and the left-lateral Dead Sea Fault Zone (DSFZ); however, previous work has indicated kinematic inconsistency between its continental and oceanic parts. The Palmyra Fold Belt (PFB) splays ENE from the DSFZ in SW Syria and persists for ~400 km to the River Euphrates, but its significance within the regional pattern of active crustal deformation has hitherto been unclear. We report deformation of Euphrates terraces consistent with Quaternary right-lateral transpression within the PFB, indicating anticlockwise rotation (estimated as 0.3° Ma^{-1} about 36.0°N 39.8°E) of the block between the PFB and the northern DSFZ relative to the Arabian Plate interior. The northern DSFZ is shown to be kinematically consistent with the combination of Euler vectors for the PFB and the Red Sea spreading, resolving the inconsistency previously evident. The SW PFB causes a significant earthquake hazard, previously unrecognized, to the city of Damascus.

Terra Nova, 21, 427–437, 2009

Introduction

The boundary between the African and Arabian plates (Fig. 1a) comprises the Red Sea oceanic spreading centre and the left-lateral Dead Sea Fault Zone (DSFZ). The northern DSFZ, in Lebanon, western Syria and southern Turkey (Fig. 1b), is transpressive, the crustal shortening that accompanies its left-lateral slip contributing to the development of local topography (e.g. Westaway, 2003; Gomez *et al*., 2006; Seyrek *et al*., 2007). The southern DSFZ is, in contrast, a good approximation to a transform fault zone. Although the kinematics of the Red Sea oceanic spreading are well constrained (e.g. Chu and Gordon, 1998), the resulting Euler vector significantly over-predicts the slip rate on the northern DSFZ (e.g. Westaway, 2003). The Palmyra Fold Belt (PFB), first described by Krenkel (1924), consisting of mountain ranges above blind reverse faults, splays ENE from the DSFZ in SW Syria and persists for ~400 km to the vicinity of the River Euphrates in NE Syria (Fig. 1b). Although the PFB exhibits relief (up to 1800 m altitude) comparable with the northern DSFZ, its development has hitherto been attributed (e.g. by Rukieh *et al*., 2005) to crustal deformation preceding the present phase, which began in the Mid-Pliocene, *c*. 3.5 Ma (e.g. Westaway *et al*., 2006, 2008a; Seyrek *et al*., 2007, 2008).

Correspondence: Rob Westaway, MCT, The Open University, Abbots Hill, Gateshead, NE8 3DF, UK. Tel.: 01913844502; e-mail: robwestaway@tiscali.co.uk

The River Euphrates crosses the line of the PFB ~40 km NW of Deir ez-Zor, its valley here flanked by the basalt-capped Halabiyeh (SW) and Kasra/Zalabiyeh (NE) plateaux (Fig. 2). Previous local descriptions of the basalts (e.g. Medvedev and Ponikarov, 1966a,b) and Euphrates terrace deposits (e.g. Besançon and Sanlaville, 1981; Sanlaville, 2004) have reported subhorizontal dispositions with no disruption by faulting. However, in a study of the structural geology, Litak *et al*. (1997) disclosed an oil-industry seismic section showing faulting reaching the Earth's surface within the bedrock SW of the Euphrates valley (Fig. 2); they proposed that the faulting is active and continues NE, disrupting the Kasra Plateau basalt, but provided no details. Their interpretation was disputed by Zanchi *et al*. (2002), who claimed that the evidence could not be verified in the field. The hitherto unresolved question of whether there is significant active faulting in this part of Syria prompted the present investigation.

Field evidence

We have surveyed the Euphrates terraces between Lake Assad and Deir ez-Zor (Fig. 1b) using differential GPS (Fig. 3) and Shuttle Radar Topographic Mission (SRTM) topographic imagery (see Supporting Information) to determine altitude, following the procedures described, for instance, by Westaway *et al*. (2006, 2008b). The terrace deposits typically consist of gravels overlain by sand and silt, the gravel being characterized by metamorphic and igneous clasts derived from north of the suture of the former Neotethys Ocean (Fig. 1b). They are inset against Late Miocene/Early Pliocene evaporite (mainly gypsum) interbedded with silts and gravels of the ancestral Euphrates (e.g. Medvedev and Ponikarov, 1966a,b). The study reach is dominated by an Early Holocene floodplain terrace (dated using ^{14}C by Besançon and Geyer, 2003; designated Qf0 after Sanlaville, 2004) up to 10 km wide and typically ~4 m above the river (Fig. 3). Above this are fragments of terrace QfI; at Ayash

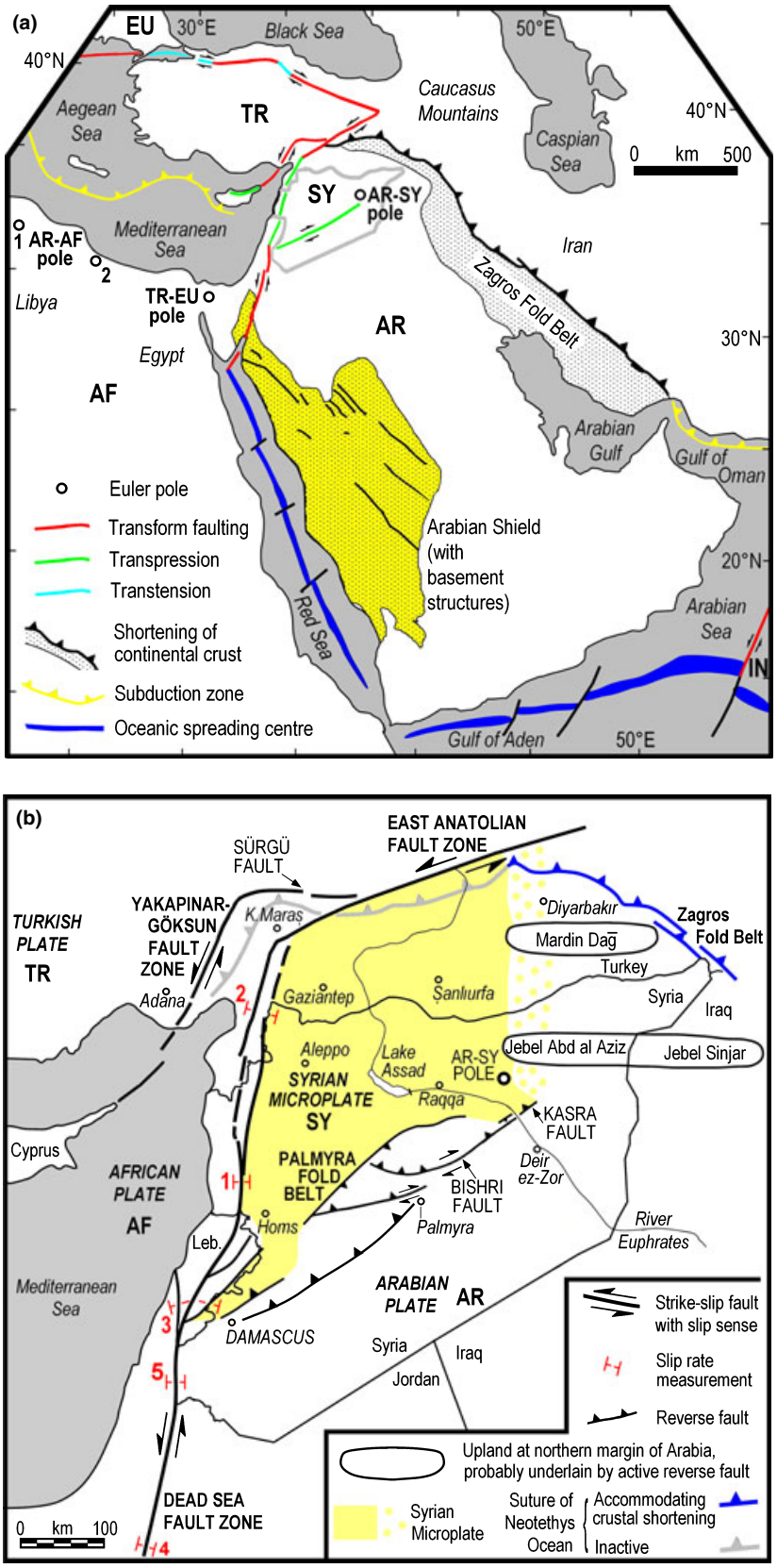

Fig. 1 Regional maps, modified after Litak *et al.* (1998). (a) Map of plate boundaries in the eastern Mediterranean and Middle Eastern region, with TR—EU Euler pole (from McClusky *et al.* 2000) and AR—SY Euler pole from this study. AR—AF pole 1, from Chu and Gordon (1998), is based on the magnetic anomalies adjoining the Red Sea oceanic spreading centre; pole 2, from Klinger *et al.* (2000), Westaway (2003) and Seyrek *et al.* (2007), fits evidence from within the DSFZ but is not consistent with this oceanic spreading. The present study shows that pole 1 fits the evidence from the northern DSFZ well, once the deformation within the PFB is taken into account. (b) Map showing active fault zones, greatly simplified, in Syria and adjoining countries, showing the extent of the Syrian microplate as envisaged in this study. Note the active anticlines, which presumably overlie blind active reverse faults, in localities north-east of the present study region. These structures represent active deformation at the northern margin of the Arabian Platform, as one approaches the broad deforming boundary zone between the Arabian and Eurasian plates (cf. Reilinger *et al.*, 2006). The relative motion between the Arabian Plate and Syrian microplate in this region, predicted from our Euler vector for the PFB, would be very slow transtension, which is not observed; we thus infer that any such motion is outweighed in this region by the component of the Arabia–Eurasia convergence that is accommodated locally. This is why the Syrian microplate is depicted as having a diffuse eastern boundary as this region of active anticlines is approached. Structural models exist that might account for the termination of a zone of localized deformation (such as, the PFB) in such a zone of distributed deformation (e.g. Froitzheim *et al.*, 2006). Further discussion of this issue is the subject of work in progress and, thus, beyond the scope of this study.

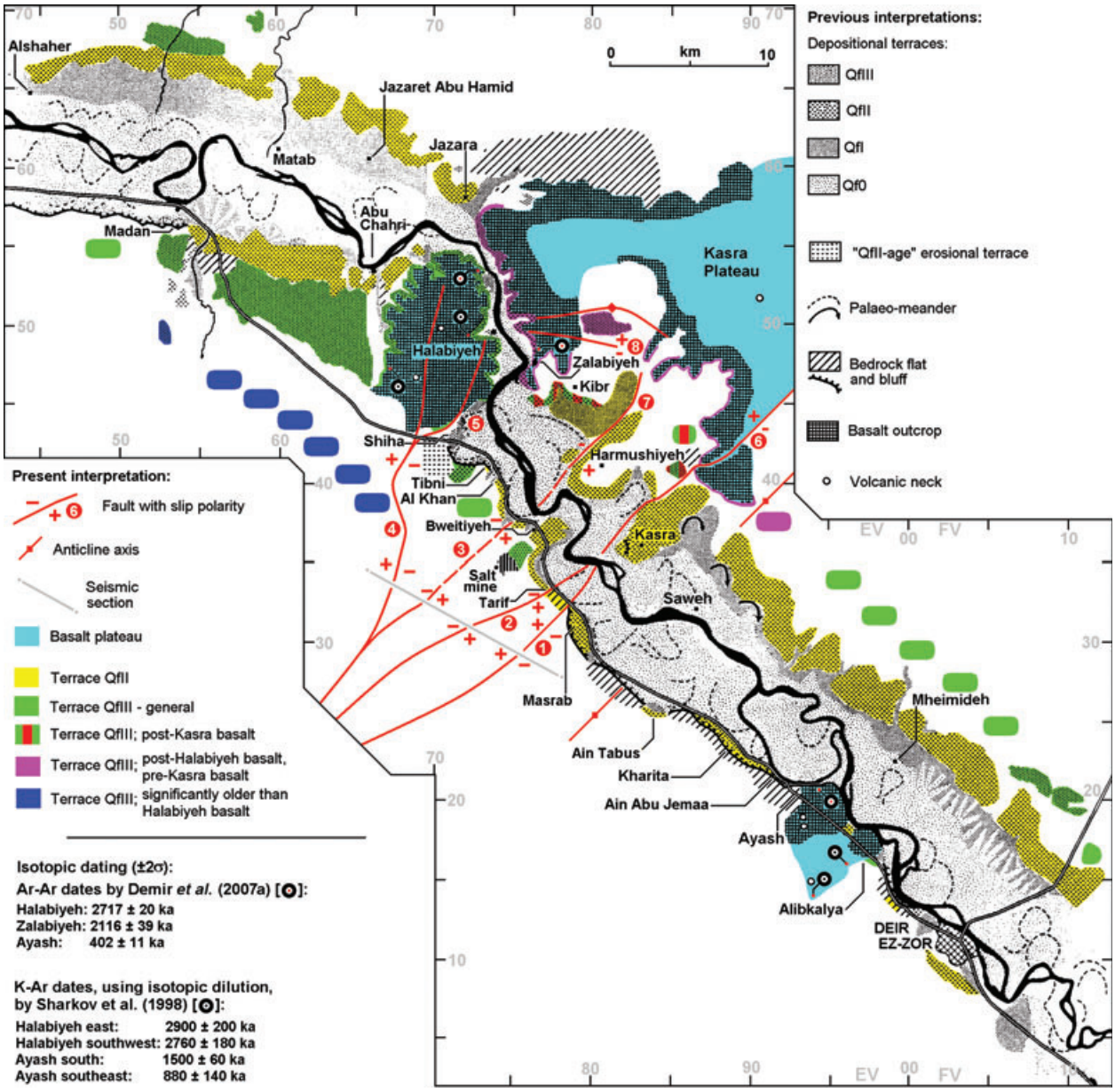

Fig. 2 Map of the study region, modified after Besançon and Sanlaville (1981) to include Universal Transverse Mercator (UTM) co-ordinates, with dating evidence from Sharkov *et al.* (1998) and Demir *et al.* (2007a) and additional information from our own fieldwork. Outcrops whose margins have not yet been mapped are illustrated schematically. The warping of the Kasra Plateau basalt along the surface trace of the Kasra Fault (6 on this map) is very clear in the field, as Litak *et al.* (1997) noted; for instance, at [EV 90049 42947] basalt in the hanging-wall of the fault is tilted SE at ~20°; basalt in the footwall is locally warped towards the fault, the line of the fault being picked out by a gulley.

(Fig. 2), these reach 9 m above present river level and are overlain by basalt, dated by Demir *et al.* (2007a) to 402 ± 11 ka. Above this, and visible along most of the valley, are much thicker and more extensive deposits of terrace QfII. In comparison with the dated terraces of the River Tigris around Diyarbakır, SE Turkey (documented by Bridgland *et al.*, 2007, and Westaway *et al.*, 2008b), this terrace is dated to *c.* 900 ka (cf. Demir *et al.*, 2008). Our fieldwork indicates that higher deposits previously grouped as terrace QfIII can be subdivided; some post-date the *c.* 2.1 Ma Kasra/Zalabiyeh basalt (dated by Demir *et al.*, 2007a), others underlie this basalt, others underlie the *c.* 2.7 Ma Halabiyeh basalt (dated by Sharkov *et al.*, 1998, and Demir *et al.*, 2007a), whereas deposits in the highest parts of the landscape significantly pre-date this older basalt (Fig. 2). The basalt capping the entire Kasra/Zalabiyeh plateau has been attributed to a single eruption phase (e.g. Medvedev

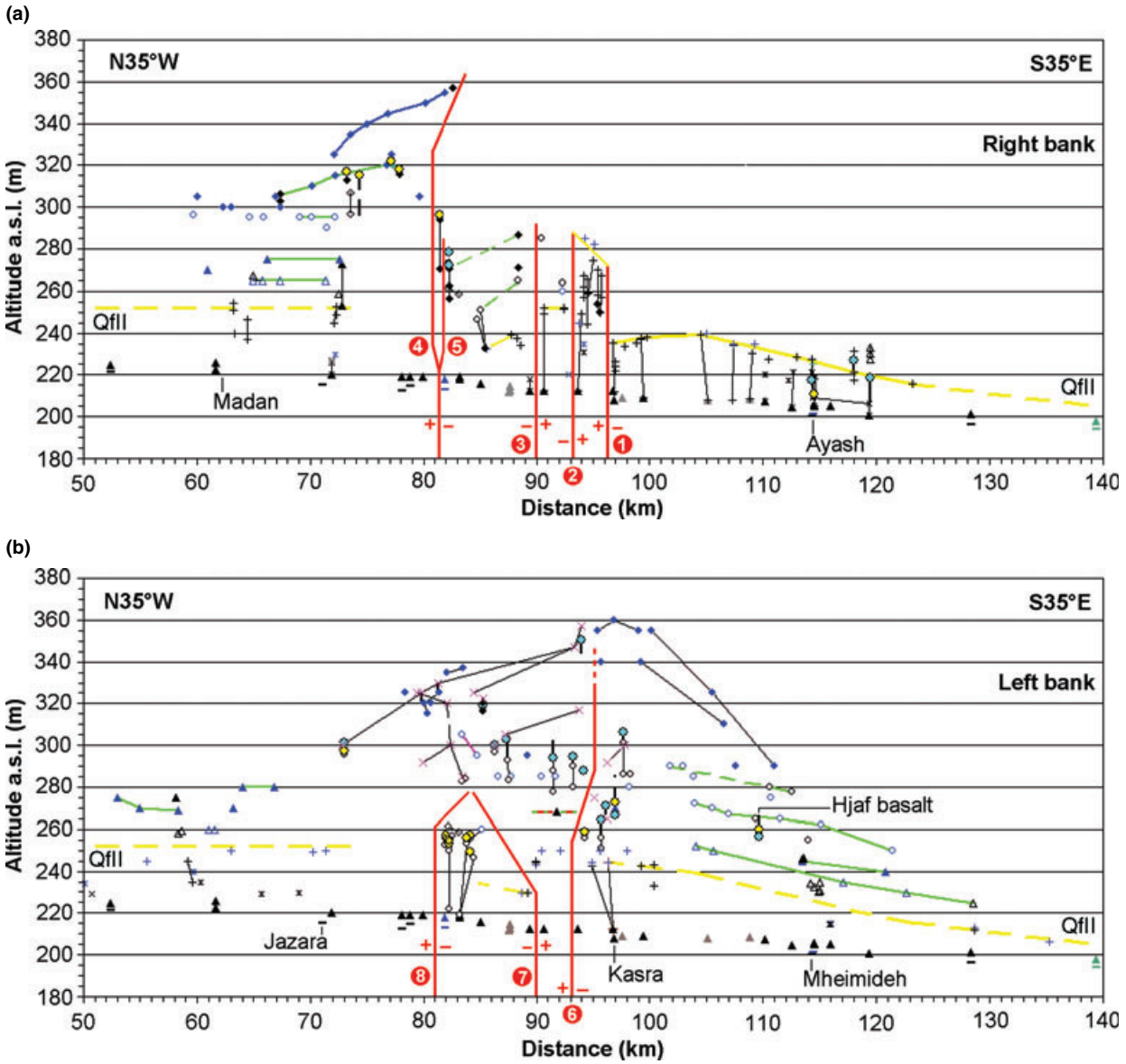

Fig. 3 Cross-sections showing variations in heights of Euphrates terraces and associated basalts on the right side (a) and left side (b) of the river. Both projections are oriented N35°W–S35°E with distance measured from an origin at UTM co-ordinates [DV 65000 70000]; terraces are labelled using the same ornament as in Fig. 2.

and Ponikarov, 1966a,b), a view supported by the geochemical similarity of the basalt throughout this area (Fig. 4).

The terraces in this reach of the Euphrates are unusual in that they are not parallel with the modern floodplain, variations in height being most clearly evident for terrace QfII (Fig. 3). For >20 km upstream of the Halabiyeh Plateau, this terrace maintains a near-constant altitude of ~250 m a.s.l., thus diverging downstream from ~30 to ~40 m above the river, while the oldest spreads of terrace QfIII are back-tilted significantly. Conversely, in the ~20 km downstream from Ain Tabus, terrace QfII falls from ~35 to ~10 m (Fig. 3a).

We also note abrupt, highly localized variations in the height of terrace QfII. Thus, in the ~8 km upstream from Ain Tabus to Masrab, it falls from ~35 to ~30 m above the Euphrates. At the western edge of Masrab, it then rises abruptly to ~60 m (Fig. 3a) as the terrace and underlying gypsum are offset across a reverse fault (Figs 5 and 6). In the ~2 km upstream of Masrab, the terrace rises to ~80 m (Fig. 5b) at Tarif, where it then falls to ~45 m in a few tens of metres; the terrace deposits and underlying bedrock are here locally tilted at up to ~25°, indicating a blind reverse fault in the subsurface. These Masrab and Tarif faults (1 and 2 in Figs 2 and 3a) are aligned with counterparts with equivalent slip polarity on the Litak *et al.* (1997) seismic section, 4–5 km farther SW (Fig. 2).

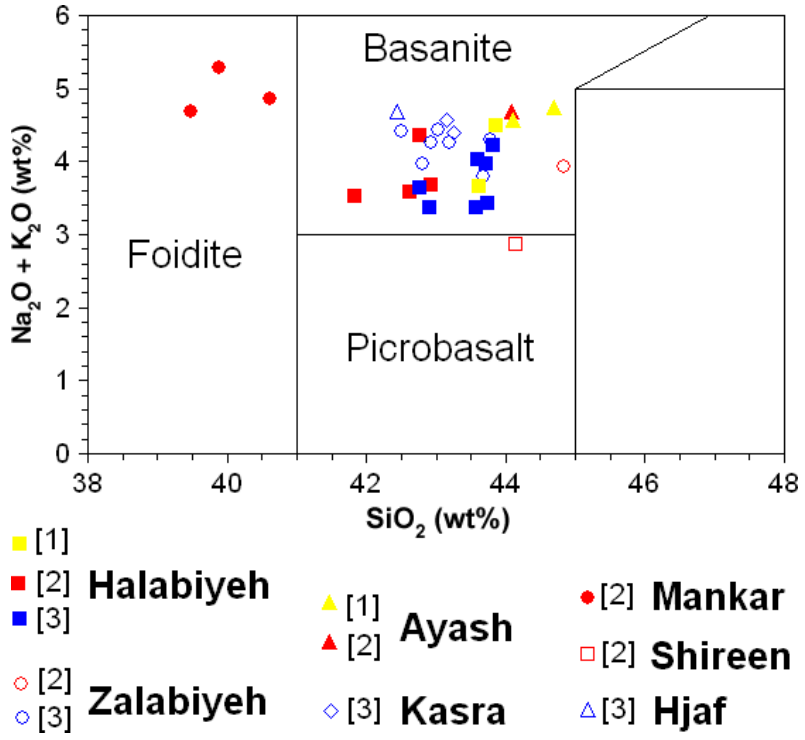

Fig. 4 Graph of percentage composition by weight of alkali metal oxides against silica for basalts from the study area, also showing standard classification fields. Symbol shapes indicate volcanic fields, their shades indicating the reference source: [1], Lustrino and Sharkov (2006); [2], Demir *et al.* (2007a); [3], this study. The plot demonstrates significant differences in composition between basalts from different eruptive centres and that the Zalabiyeh Plateau and Kasra Plateau basalts are indistinguishable, confirming that both came from a single eruptive phase of the same volcanic neck. Full geochemical analyses of the basalt samples in group [3] are provided in the Supporting Information.

Between Bweitiyeh and Al Khan, terrace QfII falls (upstream) from ~45 to ~35 m, in line with another fault in the seismic section. We thus project this, the Bweitiyeh Fault (3 in Fig. 2), to the Euphrates. A fourth fault evident in the seismic section, with downthrow to the SE, adjoins the southern end of a bluff across which the highest spread of back-tilted Euphrates gravel is abruptly truncated as the land surface drops from ~150 to ~90 m above the modern river. We attribute this to downthrow across this Tibni Fault (4 in Fig. 2). This bluff passes end-on into the southern Halabiyeh Plateau, where it marks a ~20 m displacement (from ~315 to ~295 m a.s.l.) in the contact between fluvial terrace deposits and overlying basalt. In the SE corner of the plateau, the base of the basalt is even lower, ~275 m a.s.l.; we attribute this additional displacement to downthrow on the Shiha Fault (5 in Fig. 2), which we envisage as splaying from the Tibni Fault as indicated in Fig. 2. In these localities, no faulting is visible, but the basalt is warped (Fig. 7), thus indicating (like at Tarif) blind faulting in the subsurface.

On the left side of the Euphrates, terrace QfII rises gradually upstream from ~10 m east of Deir ez-Zor to ~40 m at Kasra (Fig. 3b). Higher-level spreads of gravel, assigned to terrace QfIII, and flats in bedrock gypsum show corresponding height variations. In contrast, the contact between the basalt capping the SE Kasra Plateau and the underlying fluvial gravel tilts NW (Fig. 3b), falling gradually upstream from ~300 to ~255 m a.s.l. in ~4 km before rising abruptly to 290 m a.s.l.. Because of cover by talus, no fault is visible in the plateau bluff, but within the plateau, the basalt is clearly warped across this discontinuity, indicating the presence of the Kasra Fault (6 in Fig. 2), as previously inferred (Litak *et al.*, 1997; see also Alsdorf *et al.*, 1995). The downthrow across this fault dies out progressively north-eastward; 10 km farther NE, the plateau basalt NW of the fault line is at the same level as gypsum bedrock to the south-east. We infer that, to the SW, the Kasra Fault splays into the Masrab and Tarif faults as indicated in Fig. 2.

NW of Harmushiyeh, the surface of terrace QfII steps down abruptly from ~245 to ~230 m a.s.l., much of this extensive feature having hitherto been regarded (e.g. Besançon and Sanlaville, 1981; Sanlaville, 2004) as part of terrace QfI because of its low altitude (~20 m above river level). We attribute this instead to downthrow across the Harmushiyeh Fault (7 in Fig. 2), interpreted as a NE continuation of the Bweitiyeh Fault. Finally, localized deformation is also evident in the southern Zalabiyeh Plateau and westernmost Kasra Plateau. The Zalabiyeh plateau basalt is typically subhorizontal, reaching ~310 m a.s.l.; south of an anticline axis (indicated in Fig. 2), it tilts southward, declining to ~290 m a.s.l. in ~1–2 km. South of this point, it drops more abruptly to ~265 m a.s.l., indicating another fault (the Kibr Fault; 8 in Fig. 2), beyond which it slopes southward to ~250 m a.s.l. or only ~35 m above the Euphrates.

Sense and rate of crustal deformation

The overall effect of this deformation is to create a localized zone of maximum uplift between Masrab and Tarif, downstream of a localized zone of minimum uplift encompassing the Tibni–Kibr area, the southernmost Zalabiyeh Plateau and the extreme SE Halabiyeh Plateau. Structural evidence (e.g. Litak *et al.*, 1997; Seber *et al.*, 2000) indicates that the deformation is primarily right-lateral with a minor component of shortening (see Supporting Information, which includes discussion of the available earthquake focal mechanisms in this deforming zone). Evidence for right-lateral slip is provided by the apparent ~200 m offset of the inner edge of Euphrates terrace QfII at Tarif (Fig. 6) which, given the age of this

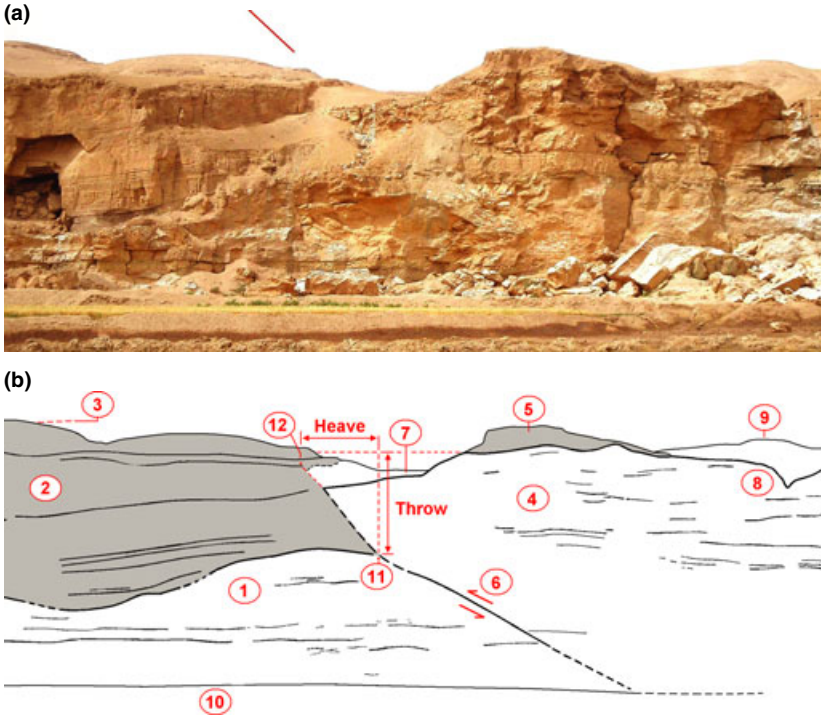

Fig. 5 (a) Field photograph looking S30°W from [EV 79098 32580] at the ~40 m high bedrock gypsum bluff capped by deposits of Euphrates terrace QfII NW of Masrab (1 in Fig. 3a; precise location at A in Fig. 6). The terrace deposits and underlying bedrock are warped and offset across the Masrab Fault. (b) Annotated sketch of (a), identifying key details, with deposits of Euphrates terrace QfII that are exposed in the terrace bluff shaded. 1, 2 and 3 are the bedrock gypsum, fluvial terrace deposits (silt, sand and gravel) and surface of fluvial terrace QfII, respectively, in the footwall of the fault. 4 and 5 are the bedrock gypsum and an outlier of the basal part of the QfII fluvial succession in its hanging-wall. 6 is the fault plane. 7 is talus derived from the fluvial deposits, which has cascaded down a gulley in the surface of the bedrock gypsum close to the footwall cutoff, partly covering the gypsum, some of which has been locally eroded. 8 is another gulley cut into the bedrock gypsum by a wadi that drains part of the QfII fluvial terrace in the hanging-wall of the fault. 9 is the surface of the QfII fluvial terrace in the middle distance (>~100 m away), away from the terrace bluff in the hanging-wall, the bulk of the fluvial deposit at closer localities in the hanging-wall having been lost to erosion. 10 is the surface of the Holocene (Qf0) floodplain terrace. 11 is the footwall cutoff of the top of the bedrock gypsum. 12 is the estimated position of the hanging-wall cutoff of the top of the bedrock gypsum, taking into account the local loss of some of this bedrock to erosion (see 7, above). Also shown are construction lines for estimating the heave and throw on the fault; these are ~15 m and ~20 m respectively. However, the resulting throw underestimates the observed ~30 m decrease in altitude of the terrace surface over a ~100-m distance (Fig. 3a). It is thus concluded that the slip on the fault decreases upward in the shallow subsurface and that the heave and throw at shallow depths (assumed to decrease in proportion) are ~23 m and ~30 m (Table 1).

terrace, indicates a slip rate of ~0.2 mm a^{-1}. The overall crustal shortening rate consistent with the field evidence between Masrab and the Halabiyeh Plateau is estimated as ~0.1 mm a^{-1} (Table 1).

Right-lateral transpression characterizes the PFB SW of the present study region, more intense deformation in this sense being evident (e.g. Litak *et al.*, 1997; Brew *et al.*, 2003), although the lack of points of reference has prevented quantification of its rate. Although modest, the deformation rates estimated from our study provide a basis for quantification throughout this zone. The evident north-eastward tapering in deformation suggests that the PFB is characterized by an Euler pole (for anticlockwise rotation of the block to the NW, which we call the Syrian microplate in Fig. 1, relative to the Arabian Plate to the south-east) located not far north of the present study region. A pole at 36.0°N, 39.8°E, with a rotation rate of 0.3° Ma^{-1}, can roughly account for the available evidence (Figs 6 and 8a).

This Euler vector for the PFB can be used, along with that for the Red Sea oceanic spreading (from Chu and Gordon, 1998), to predict the kinematics of the northern DSFZ (Figs 8 and 9). The anticlockwise rotation of the Syrian microplate relative to Arabia reduces the slip rate below that predicted from the oceanic spreading alone, bringing it into agreement with observations (e.g. those reported by Meghraoui *et al.*, 2003; and Seyrek *et al.*, 2007; Fig. 8). This implies that the PFB has the effect of absorbing part (estimated in Fig. 8 as ~20%) of the northward motion of Arabia relative to Africa that is required to accommodate the Red Sea spreading. The PFB is thought to mark an ancient line of weakness within the Arabian Platform; it was a zone of crustal extension in the Mesozoic and may also mark a boundary between terranes that sutured together in the latest Precambrian when this crust became consolidated (e.g. Litak *et al.*, 1997; Brew *et al.*, 2003). Reactivation of this zone can now be seen to be an essential element in the post-3.5 Ma geometry of the regional kinematics, enabling the northern DSFZ to slip at the observed rate, given the rate of oceanic spreading in the Red Sea. The proposed kinematic model predicts a maximum of ~9 km of crustal shortening in the SW PFB during this phase of deformation (calculated as *c.* 3.5 Ma × 2.5 mm a^{-1}; after Fig. 8a). Structural analysis by Chaimov *et al.* (1990) indicates a maximum of 20–25 km of crustal shortening in the SW PFB; much of the shortening within this zone thus pre-dates this phase of deformation.

An important implication of this analysis concerns the earthquake hazard to Damascus. This city (population ~3 000 000) is located within the SW PFB on alluvium of the

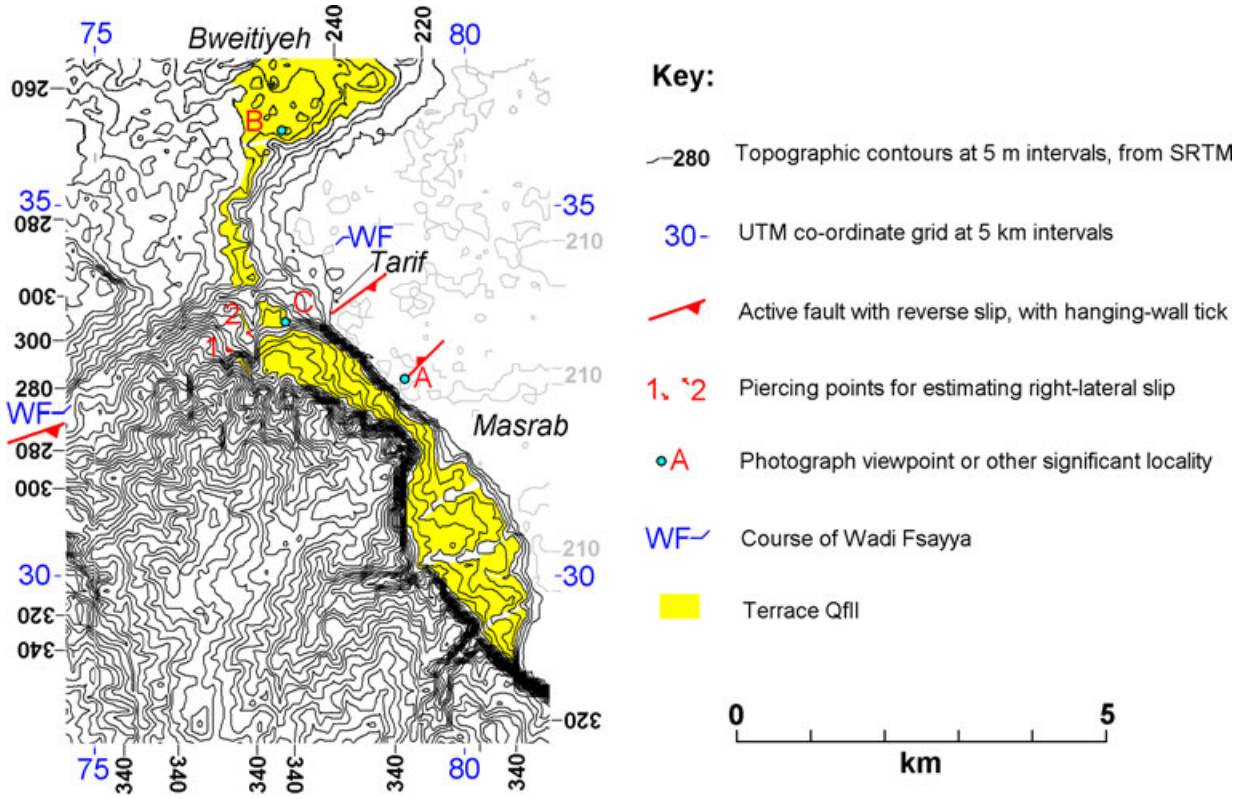

Fig. 6 Topographic map of the Bweitiyeh–Tarif–Masrab area of the right side of the Euphrates valley, showing the disposition of terrace QfII in relation to the active faults that are interpreted in this study. The topographic imagery, prepared as described by Westaway *et al.* (2006), is based on SRTM data and thus cannot resolve features with dimensions smaller than ~90 m. The WSW–ENE-striking Tarif fault, with downthrow to the NNW, follows the course of Wadi Fasayya, which joins the Euphrates valley north of Tarif. South of Bweitiyeh, terrace QfII forms a ~2 km wide flat at ~350 m a.s.l., on the inside of a meander loop, with older terrace deposits at higher levels farther west. North of Tarif, terrace QfII can be traced as a much narrower flat around the outside of another meander loop, as shown. It resumes south of Wadi Fasayya, reaching the line of the Tarif Fault at locality 2, adjoining a tributary gulley that enters the right bank of the wadi. At locality 2, a narrow flat bounded by a bluff is evident west of this gulley, circa [EV 7705 3330]; we interpret this as the inner edge of terrace QfIII NNW of the fault. SSE of the fault terrace QfII is higher, ~385 m a.s.l., because of the component of vertical slip on the fault. A narrow terrace flat can again be traced west of the tributary gulley, as far as locality 1, circa [EV 7700 3295], and is interpreted as the inner edge of the terrace in the hanging-wall of the fault. We project the inner edge of the terrace in the footwall south–south-eastward to the footwall cutoff circa [DB 7715 3310]. The ~200 m distance between these points ([EV 7700 3295] and [EV 7715 3310]) indicates ~200 m of right-lateral slip on the Tarif Fault since the end of aggradation of the deposits now forming terrace QfII, as noted in the text. The tributary gulley and wider terrace flat on its right side also appear offset right-laterally by ~200 m, but the offset of the inner edge of the terrace provides stronger evidence. Note also the much greater height of terrace QfII in the hanging-wall of the Masrab Fault than in its footwall (~285 m against ~240 m a.s.l.), because of the component of reverse slip on this fault. A field photograph illustrating the landscape in this area (looking SSE from locality B at [EV 77387 35614], near Bweitiyeh) was published as Fig. S1(d) of Demir *et al.* (2007b) and so is not repeated here. This photograph shows both the vertical and right-lateral offsets of the inner edge of terrace QfII, although this was not realized at the time; what is now apparent as the high part of terrace QfII between Tarif and Masrab was thought to be an older fluvial terrace, above the level of terrace QfII at Bweitiyeh. This high terrace flat was mapped as bedrock by Besançon and Sanlaville (1981) (Fig. 2), but is covered by Euphrates terrace deposits, now well-exposed in many localities as a result of quarrying. These terrace deposits and the underlying bedrock can be seen to be warped and tilted along the line of the Tarif Fault, for instance, beneath Tarif village between [EV 78216 33571] and [EV 77501 33445] (locality C), indicating that a single deformed fluvial terrace is present rather than two terraces at different levels as Demir *et al.* (2007b) thought.

Damascus Basin in the footwall of one of the reverse faults within this zone (the Damascus Fault; see Supporting Information) the hanging-wall of which rises ~400 m above the city (e.g. Sharkov *et al.*, 1994). The ~600 m thickness of Pliocene/Pleistocene alluvium in the Damascus Basin (dated, using interbedded basalt, after Mouty *et al.*, 1992; and Sharkov *et al.*, 1994; see Supporting Information) indicates that this fault has developed a throw of ~1000 m on this time scale, implying (assuming the motion started at 3.5 Ma) a vertical slip rate of ~0.3 mm a^{-1}. This and other reverse faults forming the SW PFB have hitherto been regarded as inactive (e.g. by Rukieh *et al.*, 2005), but our reanalysis, which predicts an overall rate of crustal shortening

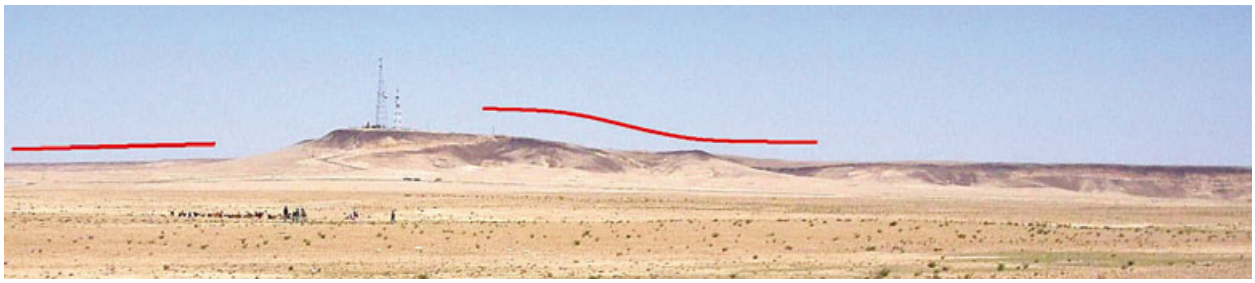

Fig. 7 Field photograph of warped basalt inferred to overlie a blind reverse fault. View N from [EV 68765 41202] to the southern tip of the Halabiyeh Plateau, showing down-to-the-east warping of the Halabiyeh basalt across the Tibni Fault and back-tilting of Euphrates gravel, overlain by the basalt, to the west of the fault.

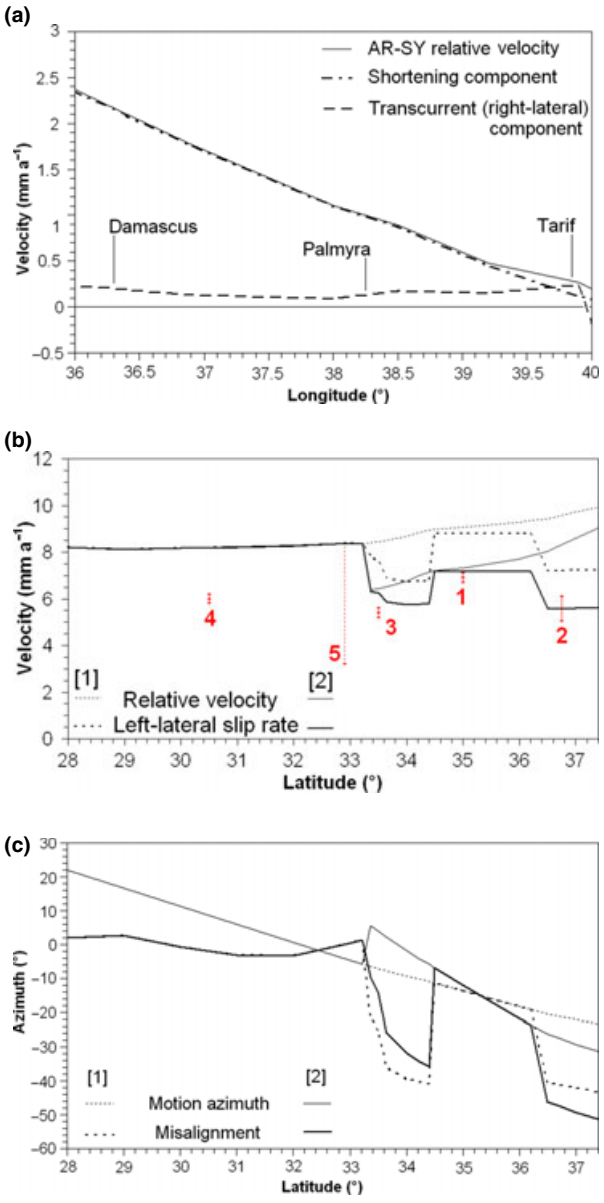

Fig. 8 Summary of proposed regional kinematic model. (a) Kinematics of the PFB predicted using the Euler vector (0.3° Ma^{-1} about 36.0°N, 39.8°E) deduced in this study. Predicted rates of motion (b) and azimuths (c) for the DSFZ, showing both the prediction using the Africa–Arabia Euler vector from Chu and Gordon (1998) [1] and the revised solution using this Euler vector in combination with that, illustrated in (a), for the PFB [2]. Observational evidence for comparison (locations in Fig. 1b) is; (1) from the Misyaf area (Meghraoui *et al.*, 2003), for slip in earthquakes in the past *c.* 2000 years; (2) from the Karasu Valley (Seyrek *et al.*, 2007), from offsets of dated Middle Pleistocene basalt flows; (3) from the Lebanon/Syria border region, for a compilation of data (Seyrek *et al.*, 2007); (4) the 6 mm a^{-1} upper bound to the left-lateral slip rate estimated south of the Dead Sea (Klinger *et al.*, 2000); and (5) the 3.2 mm a^{-1} slip rate estimated on one strand of the northernmost part (in the Jordan valley north of Lake Kinneret, at the western margin of the Jaulan region of SW Syria) of the southern DSFZ (Marco *et al.*, 2005). (4) may underestimate the overall slip rate because the southern DSFZ consists of multiple en echelon strands that straddle sensitive international borders. (5) clearly underestimates the total slip rate, as Marco *et al.* (2005) mentioned other active left-lateral faults en echelon to the one that they studied, and so is depicted with an indeterminate upper bound equal to the predicted local slip rate. In (c), misalignment means the difference in azimuth between the predicted plate motion and the active faulting, negative values indicating transpression.

Table 1 Estimation of rates of crustal shortening.

Fault	Offset marker: Name	Age (Ma)	Throw (m)	Dip (°)	Heave (m)		Rate of increase of heave (mm a^{-1})
Right side of Euphrates valley							
Masrab Fault	Top of terrace QfII	0.9 [1]	30 [2]	50 [2]	23 [2]		0.026
Tarif Fault	Top of terrace QfII	0.9 [1]	35	45 [3]	35		0.039
Bweitiyeh Fault	Top of terrace QfII	0.9 [1]	10	45 [3]	10		0.011
Tibni Fault [4]	Top of oldest Euphrates gravel	3.0 [1]	60	45 [3]	60		0.020
						Total	0.096
Halabiyeh Plateau							
Tibni Fault [5]	Halabiyeh basalt	2.7 [6]	20	45 [3]	20		0.007
Shiha Fault	Halabiyeh basalt	2.7 [6]	20	45 [3]	20		0.007
						Total	0.014 [7]
Left side of Euphrates valley							
Kasra Fault	Kasra/Zalabiyeh basalt	2.1 [6]	35	45 [3]	35		0.017
Harmushiyeh Fault	Top of terrace QfII	0.9 [1]	15	45 [3]	15		0.017
Kibr Fault	Kasra/Zalabiyeh basalt	2.1 [6]	25	45 [3]	25		0.012
						Total	0.046 [8]

Time-averaged rates of increase of heave, regarded as proxies for rates of crustal shortening across each fault, are calculated for each fault by dividing the heave by the age of the offset marker.
[1] Age estimated from regional correlations of fluvial terraces, supported by isotopic dating in the Diyarbakır area (Bridgland *et al.*, 2007; Westaway *et al.*, 2008b); [2] Throw and heave observed in the field at the fault plane (Fig. 5), but scaled to the total offset of the terrace surface. Dip calculated as $\tan^{-1}$(throw/heave); [3] Nominal dip value assumed; heave estimated as throw (estimated to the nearest 5 m from SRTM imagery) divided by tan(dip); [4] The part of the Tibni Fault SW of Tibni; [5] The part of the Tibni Fault in the southern Halabiyeh Plateau; [6] Age estimated from Ar–Ar dating of local basalt (Demir *et al.*, 2007a, and Fig. 2); [7] Shortening rate comparable to, but less than, that estimated across the Tibni Fault south of the Halabiyeh Plateau; [8] Estimated shortening rate decreases by more than 50% from that for the right side of the Euphrates valley in ~12 km distance, consistent with increasing proximity to the Euler Pole for the Palmyra Fold Belt.

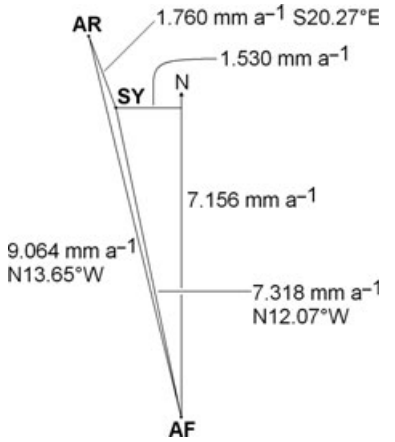

Fig. 9 Velocity vector diagram for Misyaf on the northern DSFZ in NW Syria (35.0°N, 36.3°E; locality 1 in Fig. 1b). AR-AF relative motion is calculated using the Chu and Gordon (1998) Euler vector for the Red Sea oceanic spreading centre. SY–AR relative motion is calculated using the Euler vector for the Palmyra Fold Belt from the present study. The predicted anticlockwise rotation of SY relative to AR means that the SY–AF relative motion is subparallel to, but less than, the AR–AF relative motion. The SY–AF relative motion, which is taken up on the north–south-striking northern DSFZ, can be resolved into a N–S component of ~7 mm a^{-1}, consistent with the Meghraoui *et al.* (2003) slip rate estimate and an E–W component of ~1.5 mm a^{-1}, which is accommodated by local crustal shortening (in the direction perpendicular to the northern DSFZ) across the Jebel Nusayriyah mountain range west of the northern DSFZ (cf. Westaway, 2003). In lieu of a series of other vector diagrams for different parts of the DSFZ, the results of this study are presented graphically in Fig. 8.

across this fault zone in the Damascus area of ~2 mm a^{-1} (Fig. 8a), suggests otherwise. Damascus is known to have repeatedly experienced destructive earthquakes during the past >3000 years, hitherto attributed (e.g. by Sbeinati *et al.*, 2005) to the DSFZ, which runs >40 km west of the city (Fig. 1b). Our findings imply that some of them involved slip on the Damascus Fault or other reverse faults closer to the city. Destructive earthquakes are known to have affected the PFB; for example, the ancient city of Palmyra was damaged to seismic intensities of VII and VIII respectively in AD 1043 and 1089 (Sbeinati *et al.*, 2005). Moreover, the sparseness of the population in this desert region makes it probable that other earthquakes up to magnitude 6.5 have been missed from the historical record (Sbeinati *et al.*, 2005), leading to the underestimation of the significance of the PFB that our present analysis seeks to redress.

Conclusions

Deformation of Euphrates terraces in NE Syria indicates Quaternary right-lateral transpression within the PFB. The PFB thus accommodates clockwise rotation of the Arabian Plate relative to the Syrian microplate to the NW. The kinematics of the northern DSFZ (the western boundary of the Syrian microplate) are shown to be consistent with the combination of Euler vectors for the PFB and for the Red Sea spreading, resolving the inconsistency previously evident with the relative motion across the PFB not taken into account. As a result of its proximity, the SW PFB causes a significant earthquake hazard, previously unrecognized, to the city of Damascus.

Acknowledgements

Fieldwork was funded by the Council for British Research in the Levant (D.B.) and by the Syrian National Earthquake Center. Analysis of basalt samples was funded by the British Geological Survey (S.L.). We thank Michele Lustrino and the late Professor Andrei Dodonov for helpful discussions and correspondence as well as Mustapha Meghraoui and an anonymous reviewer for their thoughtful and constructive comments.

References

Alsdorf, D., Barazangi, M., Litak, R., Seber, D., Sawaf, T. and Al-Saad, D., 1995. The intraplate Euphrates fault system-Palmyrides mountain belt junction and relationship to Arabian plate boundary tectonics. *Annali di Geofisica*, **38**, 385–397.

Besançon, J. and Geyer, B., 2003. La géomorphologie de la basse vallée de l'Euphrate Syrien. In: *La Basse Vallée de l'*Euphrate Syrien du Néolithique a l'avenement de l'Islam, Vol. 1 (B. Geyer and J.-Y. Montchambert, eds), pp. 7–59. Institut Français du Proche Orient, Beirut, Lebanon.

Besançon, J. and Sanlaville, P., 1981. Aperçu géomorphologique sur la vallée de l'Euphrate Syrien. *Paléorient*, **7**, 5–18.

Brew, G., Best, J., Barazangi, M. and Sawaf, T., 2003. Tectonic evolution of the NE Palmyride mountain belt, Syria: the Bishri crustal block. *J. Geol. Soc. Lond.*, **160**, 677–685.

Bridgland, D.R., Demir, T., Seyrek, A., Pringle, M., Westaway, R., Beck, A.R., Rowbotham, G. and Yurtmen, S., 2007. Dating Quaternary volcanism and incision by the River Tigris at Diyarbakır, SE Turkey. *J. Quatern. Sci.*, **22**, 387–393.

Chaimov, T., Barazangi, M., al-Saad, D., Sawaf, T. and Gebran, A., 1990. Crustal shortening in the Palmyride fold belt, Syria, and implications for movement along the Dead Sea fault system. *Tectonics*, **9**, 1369–1386.

Chu, D. and Gordon, R.G., 1998. Current plate motions across the Red Sea. *Geophys. J. Int.*, **135**, 313–328.

Demir, T., Westaway, R., Bridgland, D., Pringle, M., Yurtmen, S., Beck, A. and Rowbotham, G., 2007a. Ar-Ar dating of Late Cenozoic basaltic volcanism in northern Syria: implications for the history of incision by the River Euphrates and uplift of the northern Arabian Platform. *Tectonics*, **26**, 30, doi: 10.1029/2006TC001959.

Demir, T., Westaway, R., Seyrek, A. and Bridgland, D., 2007b. Terrace staircases of the River Euphrates in southeast Turkey, northern Syria and western Iraq: evidence for regional surface uplift. *Quatern. Sci. Rev.*, **26**, 2844–2863.

Demir, T., Seyrek, A., Westaway, R., Bridgland, D. and Beck, A., 2008. Late Cenozoic surface uplift revealed by incision by the River Euphrates at Birecik, southeast Turkey. *Quatern. Int.*, **186**, 132–163.

Froitzheim, N., Pleuger, J. and Nagel, T.J., 2006. Extraction faults. *J. Struct. Geol.*, **28**, 1388–1395.

Gomez, F., Khawlie, M., Tabet, C., Darkal, A.N., Khair, K. and Barazangi, M., 2006. Late Cenozoic uplift along the northern Dead Sea transform in Syria and Lebanon. *Earth Planet. Sci. Lett.*, **241**, 913–931.

Klinger, Y., Avouac, J.P., Abou Karaki, N., Dorbath, L., Bourles, D. and Reyss, J.L., 2000. Slip rate on the Dead Sea transform fault in northern Arava Valley (Jordan). *Geophys. J. Int.*, **142**, 755–768.

Krenkel, E., 1924. Der Syrische Bogen. *Cent. Miner. Geol. Palaeontol., v. Abh. B*, **9–10**, 274–281 and 301–313.

Litak, R.K., Barazangi, M., Beauchamp, W., Seber, D., Brew, G., Sawaf, T. and Al-Youssef, W., 1997. Mesozoic-Cenozoic evolution of the intraplate Euphrates fault system, Syria; implications for regional tectonics. *J. Geol. Soc. Lond.*, **154**, 653–666.

Litak, R.K., Barazangi, M., Brew, G., Sawaf, T., al-Imam, A. and al-Youssef, W., 1998. Structure and evolution of the petroliferous Euphrates graben system, southeast Syria. *AAPG Bull.*, **82**, 1173–1190.

Lustrino, M. and Sharkov, E., 2006. Neogene volcanic activity of western Syria and its relationship with Arabian plate kinematics. *J. Geodyn.*, **42**, 115–139.

Marco, S., Rockwell, T.K., Heimann, A., Frieslander, U. and Agnon, A., 2005. Late Holocene activity of the Dead Sea Transform revealed in 3D palaeoseismic trenches on the Jordan Gorge segment. *Earth Planet. Sci. Lett.*, **234**, 189–205.

McClusky, S., Balassanian, S., Barka, A., Demir, C., Ergintav, S., Georgiev, I., Gurkan, O., Hamburger, M., Hurst, K., Kahle, H., Kastens, K., Kekelidze, G., King, R., Kotzev, V., Lenk, O., Mahmoud, S., Mishin, A., Nadariya, M., Ouzounis, A., Paradissis, D., Peter, Y., Prilepin, M., Reilinger, R., Sanli, I., Seeger, H., Tealeb, A., Toksoz, M.N., Veis, G., 2000. Global Positioning System constraints on plate kinematics and dynamics in the eastern Mediterranean and Caucasus. *J. Geophys. Res.*, **105**, 5695–5719.

Medvedev, V.Y. and Ponikarov, V.P., 1966a. Geological map of Syria, 1:200,000 scale, sheet I-37-XXII Ar-Raqqa and accompanying 56 page explanatory guide. Technoexport, Moscow, and Ministry of Industry, Syrian Arab Republic, Damascus.

Medvedev, V.Y. and Ponikarov, V.P., 1966b. Geological map of Syria, 1:200,000 scale, sheet I-37-XXIII Deir Az-Zor and I-37-XXIV Al-Buwara and accompanying 42 page explanatory guide. Technoexport, Moscow, and Ministry of Industry, Syrian Arab Republic, Damascus.

Meghraoui, M., Gomez, F., Sbeinati, R., Van Der Woerd, J., Mouty, M., Darkal, A.N., Radwan, Y., Layyous, I., al-Najjar, H., Darawcheh, R., Hijazi, F., al-Ghazzi, R. and Barazangi, M., 2003. Evidence for 830 years of seismic quiescence from palaeoseismology, archaeoseismology and historical seismicity along the Dead Sea fault in Syria. *Earth Planet. Sci. Lett.*, **210**, 35–52.

Mouty, M., Delaloye, M., Fontignie, D., Piskin, O. and Wagner, J.-J., 1992. The volcanic activity in Syria and Lebanon between Jurassic and Actual. *Schweiz. Mineral. Petrogr. Mitt.*, **72**, 91–105.

Reilinger, R., McClusky, S., Vernant, P., Lawrence, S., Ergintav, S., Cakmak, R., Ozener, H., Kadirov, F., Guliev, I., Stepanyan, R., Nadariya, M., Hahubia, G., Mahmoud, S., Sakr, K., ArRajehi, A., Paradissis, D., Al-Aydrus, A., Prilepin, M., Guseva, T., Evren, E., Dmitrotsa, A., Filikov, S.V., Gomez, F., Al-Ghazzi, R. and Karam, G., 2006. GPS constraints on continental deformation in the Africa-Arabia-Eurasia continental collision zone and implications for the dynamics of plate interactions. *J. Geophys. Res.*, **111**, 26, doi: 10.1029/2005JB004051.

Rukieh, M., Trifonov, V.G., Dodonov, A.E., Minini, H., Ammar, O., Ivanova, T.P., Zaza, T., Yusef, A., al-Shara, M. and Jobaili, Y., 2005. Neotectonic map of Syria and some aspects of Late Cenozoic evolution of the northwestern boundary zone of the Arabian plate. *J. Geodyn.*, **40**, 235–256.

Sanlaville, P., 2004. Les terraces Pléistocènes de la vallée de l'Euphrate en Syrie et dans l'extrême sud de la Turquie. *Br. Archaeol. Rep. Int. Ser.*, **1263**, 115–133.

Sbeinati, M.R., Darawcheh, R. and Mouty, M., 2005. The historical earthquakes of Syria: an analysis of large and moderate earthquakes from 1365 B.C. to 1900 A.D. *Ann. Geophys.*, **48**, 347–435.

Seber, D., Steer, D., Sandvol, E., Sandvol, C., Brindisi, C. and Barazangi, M., 2000. Design and development of information systems for the geosciences; an application to the Middle East. *GeoArabia*, **5**, 269–296.

Seyrek, A., Demir, T., Pringle, M., Yurtmen, S., Westaway, R., Beck, A. and Rowbotham, G., 2007. Kinematics of the Amanos Fault, southern Turkey, from Ar-Ar dating of offset Pleistocene basalt flows: transpression between the African and Arabian plates. In: *Tectonics of Strike-slip Restraining and Releasing Bends* (W.D. Cunningham and P. Mann, eds). *Geol. Soc. Lond. Spec. Publ.*, **290**, 255–284.

Seyrek, A., Seyrek, A., Demir, T., Pringle, M., Yurtmen, S., Westaway, R., Bridgland, D., Beck, A. and Rowbotham, G., 2008. Late Cenozoic uplift of the Amanos Mountains and incision of the Middle Ceyhan river gorge, southern Turkey; Ar-Ar dating of the Düziçi basalt. *Geomorphology*, **97**, 321–355.

Sharkov, E.V., Chernyshev, I.V., Devyatkin, E.V., Dodonov, A.E., Ivanenko, V.V., Karpenko, M.I., Leonov, Y.G., Novikov, V.M., Hanna, S. and Khatib, K., 1994. Geochronology of Late Cenozoic basalts in western Syria. *Petrology*, **2**, 385–394 [Russian original: *Petrologiya*, **2** (4), 439–448].

Sharkov, E.V., Chernyshev, I.V., Devyatkin, E.V., Dodonov, A.E., Ivanenko, V.V., Karpenko, M.I., Lebedev, V.A.,

Novikov, V.M., Hanna, S. and Khatib, K., 1998. Novye dannye po geochronologii Pozdnekainozoiskich platobazaltov severo-vostochnoi periferii Krasnomorskoi riftovoi oblasti (severnaya Siriya) [New data on the geochronology of the Late Cenozoic plateau basalt of the northeast margin of the Red Sea rift region (northern Syria)]. *Dokl. Akad. Nauk*, **358**, 96–99.

Westaway, R., 2003. Kinematics of the Middle East and Eastern Mediterranean updated. *Turk. J. Earth Sci.*, **12**, 5–46.

Westaway, R., Demir, T., Seyrek, A. and Beck, A., 2006. Kinematics of active left-lateral faulting in southeast Turkey from offset Pleistocene river gorges: improved constraint on the rate and history of relative motion between the Turkish and Arabian plates. *J. Geol. Soc. Lond.*, **163**, 149–164.

Westaway, R., Demir, T. and Seyrek, A., 2008a. Geometry of the Turkey-Arabia and Africa-Arabia plate boundaries in the latest Miocene to Mid-Pliocene: the role of the Malatya-Ovacık Fault Zone in eastern Turkey. *eEarth*, **3**, 27–35 [published online; open access] Available at: http://www.electronic-earth.net/3/27/2008/ee-3-27-2008.pdf.

Westaway, R., Guillou, H., Seyrek, A., Demir, T., Bridgland, D., Scaillet, S. and Beck, A., 2008b. Late Cenozoic surface uplift, basaltic volcanism, and incision by the River Tigris around Diyarbakır, SE Turkey. *Int. J. Earth Sci. (Geol. Rundsch.)*, **98**, 601–625.

Zanchi, A., Crosta, G.B. and Darkal, A.N., 2002. Paleostress analyses in NW Syria: constraints on the Cenozoic evolution of the northwestern margin of the Arabian plate. *Tectonophysics*, **357**, 255–278.

Received 14 October 2008; revised version accepted 2 July 2009

